

Transport through a magnetic impurity: a slave-spin approach

Daniele Guerzi¹

¹*International School for Advanced Studies (SISSA), Via Bonomea 265, I-34136 Trieste, Italy*
(Dated: June 7, 2019)

We study transport across a magnetic impurity by means of a recently developed slave-spin technique that does not require any constraint. Within a conserving mean-field approximation we find a conductance that displays both the known zero-bias anomaly but also the expected peak at bias of order U . We extend the slave-spin mean-field approximation to study the out of equilibrium transient evolution of a quantum dot. We apply the method to investigate the time-evolution of a quantum dot induced by a time-dependent electrochemical potential applied to the contacts. Similarly to the time-dependent Gutzwiller approximation, the mean-field slave-spin dynamics is able to capture dissipation in the leads, so that a steady-state is reached after a characteristic relaxation time.

I. INTRODUCTION

Originally observed in magnetic alloys¹, the Kondo effect^{2,3}, maybe the simplest collective phenomena due to strong correlations, is now routinely realized in magnetic nanocontacts, either by real magnetic atoms and molecules^{4–6} or artificial ones^{7,8}, e.g. quantum dots, and reveals itself by the so-called zero-bias anomaly^{9–12}. It arises by the coupling between a single magnetic atom, such as cobalt, and the conduction electrons of an otherwise non-magnetic metal. Such an impurity typically behaves like a local moment that, due to spin exchange, forms a many-body spin singlet state with the itinerant electrons.

Unlike magnetic alloys, nanoscale Kondo systems can be driven out of equilibrium by applying charge or spin bias voltages across the devices¹³. In such a nonequilibrium situation, the interplay between the time dynamics and strong correlation effects makes the theoretical description extremely challenging. To address this problem many innovative approaches have been developed, such as time-dependent numerical renormalization group^{14–16}, real time Monte Carlo^{17,18}, time-dependent density-matrix renormalization group^{19–21}, flow equation methods^{22–24}, perturbative renormalization group^{25–29}, time-dependent variational approaches^{30,31}, slave-particle techniques^{32–35} and exact approaches^{36,37}. Despite the rich variety of methods, they often become numerically costly at long times, which limit their application to the short times evolution of simple models. However, some of them^{31,32}, even if less accurate, are semianalytical methods able to study the full out of equilibrium evolution of realistic systems.

To the latter class of approaches belongs the nonequilibrium slave-spin technique for magnetic impurities we present in this paper. By means of a recently developed slave-spin technique³⁸, we map without any constraint a single-orbital Anderson impurity model (AIM), characterized by a particle-hole symmetric hybridization with the contacts, onto a resonant level model coupled to a single quantum pseudospin. In this suitable representation, a simple self-consistent Hartree-Fock calculation is able

to reproduce qualitatively the differential conductance of a single-orbital magnetic impurity both in the small and large bias regimes. Moreover, the slave-spin technique allows to study the full time evolution of magnetic impurities coupled with metallic leads under a nonequilibrium protocol.

The plan of the paper is as follows: we first introduce the AIM to describe a single-orbital magnetic impurity coupled with metallic contacts in section II. We then present in section II A our slave-spin mapping, which allows to compute time-dependent average values without any constraint, details are given in section II B. In section III we present the mean-field approximation for the out of equilibrium dynamics of a single-orbital magnetic impurity. Then, by assuming that the system relaxes after an initial transient, we present, in section IV, the mean-field approximation for the nonequilibrium steady-state regime. To highlight the importance of the approach presented in this work, section V is devoted to the application of the method to transport in magnetic impurities coupled with metallic contacts. In particular, in section V A, we consider the nonequilibrium steady-state induced by applying a constant voltage to the contacts. Furthermore, in section V B we compute within a self-consistent approximation scheme the steady-state differential conductance. Finally, section V C is devoted to the analysis of the out of equilibrium evolution induced by a time-dependent voltage applied to the metallic contacts. Technical points of the calculations are given in appendices A, B and C at the end of the paper.

II. THE MODEL

We model a single-orbital magnetic impurity coupled to left (L) and right (R) contacts in terms of an AIM

$$H(t; U, V_g, h) = H_{dot}(t; U, V_g, h) + H_c + T(t) \quad (1)$$

where the first term corresponds to an interacting impurity

$$H_{dot}(t; U, V_g, h) = -U\Omega/4 - V_g(t)(n - 1) - h(t)(n_\uparrow - n_\downarrow), \quad (2)$$

where d_σ is the annihilation operator of an electron state on the impurity, $n_\sigma = d_\sigma^\dagger d_\sigma$ the corresponding density, $\Omega = -(2n_\uparrow - 1)(2n_\downarrow - 1)$ and $n = n_\uparrow + n_\downarrow$. In Hamiltonian (2) U denotes the charging energy, V_g the gate potential and h the Zeeman field applied on the dot. The non-interacting leads are represented by a free electron gas with half-bandwidth D

$$H_c = \sum_{a=L,R} \sum_{k\sigma} (\epsilon_k - \phi_a) c_{ak\sigma}^\dagger c_{ak\sigma}, \quad (3)$$

where ϕ_a is the electrochemical potential that fixes the number of electrons in each contact, $\phi_L = -\phi_R$.

Finally, the tunneling coupling between the leads and the central region is represented by:

$$T(t) = \sum_{a=L,R} \sum_{k\sigma} \left(v_{ak}(t) c_{ak\sigma}^\dagger d_\sigma + H.c. \right) / \sqrt{V}, \quad (4)$$

where $v_{ak}(t)$ is a time-dependent tunneling amplitude, and V is the number of k states. In this article we limit the analysis to the symmetric case where $v_{Lk}(t) = v_{Rk}(t)$. Furthermore, we assume a particle-hole symmetric bath, i.e. for any ϵ_k there exist a k^* such that $\epsilon_{k^*} = -\epsilon_k$ and:

$$\Gamma(-\epsilon, t) = \Gamma(\epsilon, t),$$

where

$$\Gamma(\epsilon, t) = \pi \sum_k |v_k(t)|^2 \delta(\epsilon - \epsilon_k) / V. \quad (5)$$

Under a spin- σ particle-hole transformation \mathcal{C}_σ

$$\left(d_\sigma \rightarrow d_\sigma^\dagger \cup \prod_k \left(c_{Lk\sigma} \rightarrow -c_{Rk^*\sigma}^\dagger \cup c_{Rk\sigma} \rightarrow -c_{Lk^*\sigma}^\dagger \right) \right), \quad (6)$$

the Hamiltonian (1) parameters change as follows,

$$U \rightarrow -U, \quad V_g \rightarrow \mp h, \quad h \rightarrow \mp V_g, \quad (7)$$

where upper and lower signs refer to the action of \mathcal{C}_\uparrow and \mathcal{C}_\downarrow , respectively. The particle-hole transformation (6) has been defined by mixing R and L contacts to leave the electrochemical potential (3) invariant.

To study transport across the impurity is convenient to perform the Glazman-Raikh rotation¹¹:

$$\begin{pmatrix} c_{1k\sigma} \\ c_{2k\sigma} \end{pmatrix} = \frac{1}{\sqrt{2}} \begin{pmatrix} 1 & 1 \\ 1 & -1 \end{pmatrix} \begin{pmatrix} c_{Lk\sigma} \\ c_{Rk\sigma} \end{pmatrix}. \quad (8)$$

We notice that the anti-symmetric combination of the electron states in the leads $c_{2k\sigma}$ is fully decoupled from the impurity, while the symmetric combination $c_{1k\sigma}$ remains coupled to d_σ , see Eq. (4). Thus, the Kondo screening involves only the $c_{1k\sigma}$ variables. On the other hand, the current operator is expressed in terms of $c_{2k\sigma}$ only:

$$I(t) = -i \sum_\sigma \sum_k \left(v_k(t) c_{2k\sigma}^\dagger d_\sigma - H.c. \right) / \sqrt{2V}, \quad (9)$$

where the current operator, defined as $I = (I_L - I_R)/2$ and $I_a = \dot{N}_a$, is invariant under the particle-hole transformation (6).

A. The slave-spin representation

In the local magnetic regime, when U is by far the largest energy scale, charge fluctuations are well-separated in energy from spin ones. However, Hamiltonian (1) lacks a clear separation between charge and spin degrees of freedom that is desirable in the magnetic moment regime. To disentangle low and high energy sectors we enlarge the original Hilbert space \mathcal{H} by adding a single quantum pseudospin variable σ :

$$|n\rangle \rightarrow |n\rangle \otimes |s\rangle.$$

where $|n\rangle = \{|0\rangle, |\uparrow\rangle, |\downarrow\rangle, |\uparrow\downarrow\rangle\}$ and $|s\rangle = \{|+\rangle, |-\rangle\}$. Therefore, we encode valence fluctuations, measured by the operator:

$$\Omega = -(2n_\uparrow - 1)(2n_\downarrow - 1) = \begin{cases} -1 & \text{if } \{|\uparrow\downarrow\rangle, |0\rangle\}, \\ +1 & \text{if } \{|\uparrow\rangle, |\downarrow\rangle\}, \end{cases}$$

in σ^z by imposing the local constraint that filters the physical subspace out from the enlarged Hilbert space \mathcal{H}^* :

$$\langle s| \otimes \langle n| \left(\sigma^z \Omega \right) |n\rangle \otimes |s\rangle = 1.$$

Consequently, the eigenstates of σ^z refer to the presence ($|+\rangle$) or the absence ($|-\rangle$) of a local magnetic moment in the impurity site. In addition, we introduce two auxiliary fermionic operators f_σ that annihilate a pseudofermion state on the impurity. The precise relation between the original electrons and the auxiliary degrees of freedom is given by:

$$d_\sigma = \sigma^x f_\sigma \quad (10)$$

ensuring the anticommutation relations $\{d_\sigma, d_{\sigma'}^\dagger\} = \delta_{\sigma\sigma'}$. In the physical subspace, which is selected by the projector

$$\mathbb{P} = \frac{1 + \sigma^z \Omega}{2}, \quad (11)$$

the original model (1) is equivalent to:

$$H^*(t; U, V_g, h) = H_c + \sigma^x T(t) + H_{dot}^*(t; U, V_g, h), \quad (12)$$

where H_c remains unaltered, $T(t)$ is obtained by replacing d_σ with f_σ in Eq. (4), while the dot Hamiltonian is:

$$\begin{aligned} H_{dot}^*(t; U, V_g, h) = & -\frac{U}{4} \sigma^z - V_g(t)(1 - \sigma^z) \left(n_\uparrow - \frac{1}{2} \right) \\ & - h(t)(1 + \sigma^z) \left(n_\uparrow - \frac{1}{2} \right). \end{aligned} \quad (13)$$

Thus, the original Anderson impurity model is mapped into a resonant level model coupled to the pseudospin σ^x

operator in the presence of a transverse field along the σ^z component. We observe that the Hamiltonian H^* possesses a local Z_2 gauge symmetry generated by the parity transformation $\sigma^z \Omega = 2\mathbb{P} - 1$. Therefore, the quantum dynamics, induced by the operator $\sigma^x T(t)$, couples the singly occupied impurity configuration $\{|\downarrow\rangle, |\uparrow\rangle\} \otimes |+\rangle$ with $\{|0\rangle, |\uparrow\downarrow\rangle\} \otimes |-\rangle$ and does not mix physical and unphysical subspaces.

Finally, we notice that in the physical subspace the current operator reads:

$$I^*(t) = \sigma^x I(t) \quad (14)$$

where $I(t)$, defined in Eq. (9), contains f_σ pseudofermion operators.

Remarkably, the time-dependent evolution of the AIM, Eq. (1), can be obtained from the auxiliary model in Eq. (12) without any constraint on the enlarged Hilbert space. The proof of this equivalence follows the same steps of the equilibrium case, see Ref.³⁸. However, we consider valuable to show, in the next section, the possibility to remove the constraint in the time-dependent average value of the charge current, defined in Eq. (9).

B. Fate of the constraint in the dynamics

Without losing generality, we assume the model in Eq. (12) prepared at time $t = 0$ in thermal equilibrium at temperature $T = 1/\beta$:

$$\rho(U, V_g, h) = \frac{e^{-\beta H(U, V_g, h)}}{Z(U, V_g, h)},$$

where $Z(U, V_g, h) = \text{Tr}(e^{-\beta H(U, V_g, h)})$ and the impurity is decoupled from the contacts $v_k(0) = 0$. For $t > 0$ we let the system evolve by suddenly changing the coupling between the bridging region and the leads: $v_k(t > 0) = v_k$. We note that the initial distribution may include a chemical potential bias between L and R contacts. The average current flowing across the dot (9) is defined as:

$$I(t; U, V_g, h) = \text{Tr} \left[\rho(U, V_g, h) U^\dagger(t, 0; U, V_g, h) I U(t, 0; U, V_g, h) \right],$$

where U is the unitary time evolution operator. Since the trace is invariant under similarity transformations and $\mathcal{C}_\downarrow^\dagger I \mathcal{C}_\downarrow = I$, Eq. (7) implies:

$$I(t; U, V_g, h) = I(t; -U, h, V_g),$$

and

$$I(t; U, V_g, h) = \frac{I(t; U, V_g, h) + I(t; -U, h, V_g)}{2}. \quad (15)$$

Within the slave-spin representation the initial equilibrium distribution is described by

$$\rho^*(U, V_g, h) = \frac{e^{-\beta H^*(U, V_g, h)}}{Z(U, V_g, h)},$$

and the average value of the current reads

$$I(t; U, V_g, h) = \text{Tr} \left[\rho^*(U, V_g, h) (U^*)^\dagger(t, 0; U, V_g, h) \sigma^x I U^*(t, 0; U, V_g, h) \mathbb{P} \right],$$

where the trace is on the enlarged Hilbert space, \mathbb{P} , defined in Eq. (11), is the projector in the physical subspace and U^* is the time evolution operator generated by H^* . In the slave-spin representation (12) the role of the p-h symmetry transformation \mathcal{C}_\downarrow is simply played by σ^x , so

$$\begin{aligned} I(t; -U, h, V_g) &= \text{Tr} \left[\rho^*(-U, h, V_g) (U^*)^\dagger(t, 0; -U, h, V_g) \sigma^x I U^*(t, 0; -U, h, V_g) \mathbb{P} \right] \\ &= \text{Tr} \left[\rho^*(U, V_g, h) (U^*)^\dagger(t, 0; U, V_g, h) \sigma^x I U^*(t, 0; U, V_g, h) \sigma^x \mathbb{P} \sigma^x \right]. \end{aligned}$$

Eq. (15) implies:

$$\begin{aligned} 2I(t; U, V_g, h) &= \text{Tr} \left[\rho^*(U, V_g, h) (U^*)^\dagger(t, 0; U, V_g, h) \sigma^x I U^*(t, 0; U, V_g, h) \mathbb{P} \right] \\ &\quad + \text{Tr} \left[\rho^*(U, V_g, h) (U^*)^\dagger(t, 0; U, V_g, h) \sigma^x I U^*(t, 0; U, V_g, h) \sigma^x \mathbb{P} \sigma^x \right]. \end{aligned}$$

Since $1 = \mathbb{P} + \sigma^x \mathbb{P} \sigma^x$, it readily follows that:

$$I(t; U, V_g, h) = \text{Tr} \left[\frac{e^{-\beta H^*(U, V_g, h)}}{Z^*(U, V_g, h)} (U^*)^\dagger(t, 0; U, V_g, h) \sigma^x I U^*(t, 0; U, V_g, h) \right], \quad (16)$$

where we have used the equivalence $Z^*(U, V_g, h) = 2Z(U, V_g, h)$. Eq. (16) states that the time-dependent average value of the current flowing across the impurity

(1) can be computed in the slave-spin representation (12) without any constraint.

Following the same line of reasoning, previous result extends to any time-dependent average of physical observables and holds for any nonequilibrium protocol. Thus, we conclude that the out of equilibrium evolution of the original model (1) can be obtained within the slave-spin representation (12) without projecting out unphysical configurations introduced by the mapping (10).

III. TIME-DEPENDENT MEAN-FIELD EQUATIONS

In this section we present the mean-field approximation to describe the out of equilibrium evolution of a driven magnetic impurity. The dynamics of the AIM (1) is governed by the time-dependent Schrödinger equation:

$$i\partial_t|\Psi(t)\rangle = H^*(t; U, V_g, h)|\Psi(t)\rangle, \quad (17)$$

where at $t = 0$ the system is prepared in the ground state configuration $|\Psi(0)\rangle$ of the initial Hamiltonian Eq. (12).

The mean-field approach consists in approximating³⁸ the time-dependent wave function $|\Psi(t)\rangle$ with a factorized one product of a fermionic part $|\Phi(t)\rangle$ times a spin one $|\chi(t)\rangle$:

$$|\Psi(t)\rangle = |\chi(t)\rangle \otimes |\Phi(t)\rangle. \quad (18)$$

We notice that the previous approximation is appropriate in the local moment regime, i.e. $U/\Gamma \gg 1$, where the two subsystems are characterized by well-separated energy scales. This is indeed the regime we consider hereafter.

The dynamics of the interacting model (17) is, thus, reduced to the evolution of a spin degree of freedom:

$$\partial_t\langle\sigma^i(t)\rangle = -2\epsilon_{ijk}\mathcal{B}_j(t)\langle\sigma^k(t)\rangle, \quad (19)$$

under a self-consistent time-dependent magnetic field:

$$\vec{\mathcal{B}}(t) = \left(-\langle T(t) \rangle, 0, \frac{U}{4} + (h(t) - V_g(t)) \left(\langle n_\uparrow(t) \rangle - \frac{1}{2} \right) \right).$$

Eq.(19) is coupled with the Schrödinger Eq. for the Slater determinant $|\Phi(t)\rangle$:

$$i\partial_t|\Phi(t)\rangle = H_f^*(t)|\Phi(t)\rangle, \quad (20)$$

where the effective fermionic Hamiltonian is

$$H_f^*(t) = H_{leads} + \langle\sigma^x(t)\rangle T(t) - \lambda_\uparrow(t)n_\uparrow, \quad (21)$$

and $\lambda_\uparrow(t) = V_g(t)(1 - \langle\sigma^z(t)\rangle) + h(t)(1 + \langle\sigma^z(t)\rangle)$. For a given initial configuration, $|\Psi(0)\rangle = |\chi(0)\rangle \otimes |\Phi(0)\rangle$, Eqs. (19) and (20) allow to study the dynamics of the original correlated model in terms of the evolution of a spin 1/2 coupled with a time-dependent Resonant level model.

As observed in section II B, we emphasize that the nonequilibrium evolution of the Hamiltonian (1) can be

obtained by the slave-spin representation without any need of local constraints that project out unphysical configurations introduced by the mapping (10). The advantages, respect to other slave-particles approaches^{32,35}, are twofold. On one side, we reduce the number of dynamical equations. On the other side, we avoid the mean-field mixing of unphysical and physical subspaces.

The dynamical Eqs. (19) and (20) are equivalent to the ones obtained by applying the time-dependent Gutzwiller approximation (t-GA)³⁹ to the AIM³¹. In this regard, the evolution of the time-dependent Gutzwiller parameters resemble the dynamics of the spin variable, while the bath $c_{ak\sigma}$ and the pseudofermion f_σ degrees of freedom evolve under a time-dependent self-consistent Hamiltonian (21).

For large time, namely after the transient, we assume that, due to the coupling with infinite contacts, the solution of Eqs. (19) and (20) thermalizes to a steady-state. In order to describe the asymptotic regime we develop, in the next section, the nonequilibrium stationary mean-field approach.

IV. MEAN-FIELD FOR THE NONEQUILIBRIUM STEADY-STATE

In this section we discuss the mean-field approximation in the nonequilibrium steady-state.

Without losing generality, we shall assume that at $t = 0$ the contacts are disconnected to the dot but in the presence of a finite bias, so that their distribution functions read:

$$\langle c_{L(R)k\sigma}^\dagger c_{L(R)k\sigma} \rangle = f_{L(R)}(\epsilon_k) = f(\epsilon_k \mp \phi/2), \quad (22)$$

where ϕ is the voltage difference applied to the contacts and $f(\epsilon)$ is the Fermi-Dirac distribution function. Once the tunneling amplitude (4) is turned on, a time-dependent current starts to flow across the junction accordingly to Eqs. (19) and (20). For large time, namely after the transient, we assume that the system described by the ground-state $|\Psi(t)\rangle$ reaches a stationary state

$$|\Psi(t)\rangle \rightarrow |\Psi\rangle_{st}, \quad (23)$$

characterized by a constant current. We observe that Eq. (23) is a justified assumption. Indeed, as presented in section V C, the slave-spin mean-field evolution predicts, for large time, the existence of a steady-state due to the coupling of the dot with infinite contacts.

Following the same reasoning of section III, the stationary mean-field approach consists in approximating³⁸ the ground-state wave function (23) with a factorized one:

$$|\Psi\rangle_{st} = |\chi\rangle_{st} \otimes |\Phi\rangle_{st}, \quad (24)$$

where $|\Phi\rangle_{st}$ is the fermionic part and $|\chi\rangle_{st}$ the spin one. At stationarity, the pseudospin degree of freedom is con-

trolled by the Hamiltonian:

$$H_\sigma^* = -\frac{U}{4}\sigma^z + \langle T \rangle_{st} \sigma^x + (V_g - h) \left\langle n_\uparrow - \frac{1}{2} \right\rangle_{st} \sigma^z, \quad (25)$$

where $\langle \dots \rangle_{st} = \langle \Phi | \dots | \Phi \rangle_{st}$ and

$$\langle T \rangle_{st} = \sqrt{\frac{2}{V}} \sum_{k\sigma} v_k \langle f_\sigma^\dagger c_{1k\sigma} + H.c. \rangle_{st}, \quad (26)$$

$$\langle n_\uparrow \rangle_{st} = \langle f_\uparrow^\dagger f_\uparrow \rangle_{st}, \quad (27)$$

are expectation values in the fermionic steady-state wave function. The ground-state of (25) is identified by:

$$\begin{aligned} \langle \sigma^x \rangle_{st} &\equiv \sin \theta = \frac{\mathcal{B}_x / \mathcal{B}_z}{\sqrt{1 + (\mathcal{B}_x / \mathcal{B}_z)^2}}, \\ \langle \sigma^z \rangle_{st} &\equiv \cos \theta = \frac{1}{\sqrt{1 + (\mathcal{B}_x / \mathcal{B}_z)^2}}, \end{aligned} \quad (28)$$

where for convenience we have introduced the self-consistent magnetic field:

$$\mathcal{B} = \left(-\langle T \rangle_{st}, 0, \frac{U}{4} - (V_g - h) \left\langle n_\uparrow - \frac{1}{2} \right\rangle_{st} \right). \quad (29)$$

The fermionic problem is, thus, reduced to find the steady-state ground-state of the quantum Hamiltonian

$$H_f^* = H_c + \sin \theta \sum_{k\sigma} \sqrt{\frac{2}{V}} v_k \left(c_{1k\sigma}^\dagger f_\sigma + H.c. \right) - \lambda_\uparrow n_\uparrow \quad (30)$$

where $c_{1k\sigma}$ is introduced in the aforementioned unitary transformation (8) and

$$\lambda_\uparrow = h(1 + \cos \theta) + V_g(1 - \cos \theta).$$

Since we deal with a nonequilibrium situation we work in the framework of the Keldysh technique, as employed in the literature^{40–42}. Eq. (26) requires the evaluation of the lesser Green's function $G_{1kf\sigma}^<(t, t) = i \langle f_\sigma^\dagger(t) c_{1k\sigma}(t) \rangle$, which, by means of the Dyson's Eq., can be expressed in terms of the dressed Green's function of the f_σ pseudofermions and the free Green's function of the contacts. Instead, Eq. (27) can be expressed in terms of the pseudofermions Green's function only. By performing straightforward calculations, that are summarized in appendix A, we obtain:

$$\langle T \rangle_{st} = \frac{2}{\sin \theta} \sum_\sigma \int d\epsilon (\epsilon + \lambda_\sigma) f_{\text{neq}}(\epsilon) A_{f\sigma}(\epsilon), \quad (31)$$

$$\langle n_\uparrow \rangle_{st} = \int d\epsilon f_{\text{neq}}(\epsilon) A_{f\uparrow}(\epsilon), \quad (32)$$

where the nonequilibrium distribution on the impurity is $f_{\text{neq}}(\epsilon) = (f_L(\epsilon) + f_R(\epsilon))/2$ and the f_σ pseudofermion spectral function reads

$$A_{f\sigma}(\epsilon) = \frac{1}{\pi} \frac{-\text{Im} \Sigma_{f\sigma}^R(\epsilon)}{(\epsilon + \lambda_\sigma - \text{Re} \Sigma_{f\sigma}^R(\epsilon) + \text{Im} \Sigma_{f\sigma}^R(\epsilon))^2}.$$

Within the mean-field approximation, the f_σ pseudofermions self-energy is given by:

$$\Sigma_{f\sigma}^R(\omega) = 2 \sin^2 \theta \int \frac{d\epsilon}{\pi} \frac{\Gamma(\epsilon)}{\omega - \epsilon + i0^+},$$

where the factor of 2 counts the presence of two different leads, while the hybridization function $\Gamma(\epsilon)$ is defined in Eq. (5).

Given the spectral properties of the contacts, i.e. $\Gamma(\epsilon)$, Eqs. (31) and (32) give an analytic expressions for the effective magnetic field \mathcal{B} , which depends on the steady-state average $\langle \sigma^x \rangle_{st}$. Therefore, we close the set of mean-field equations and the steady-state variational ground-state is obtained by solving:

$$\sin \theta = \frac{\mathcal{B}_x(\theta) / \mathcal{B}_z(\theta)}{\sqrt{1 + (\mathcal{B}_x(\theta) / \mathcal{B}_z(\theta))^2}} \quad (33)$$

that corresponds to a root-finding problem $g(\theta) = 0$ in a single angular variable θ .

Before concluding the section, we observe that the nonequilibrium steady-state self-consistent Eq. (33) is equivalent to the one obtained with the out of equilibrium Gutzwiller approach for quantum dots⁴³. However, in comparison with the latter approach, the slave-spin method has the advantage of allowing one to use the machinery of quantum field theory, i.e. Wick's theorem, to improve mean-field results by including fluctuations.

V. APPLICATION TO TRANSPORT THOROUGH A MAGNETIC IMPURITY

The last section of this work is devoted to the application of the method, developed in sections III and IV, to study the nonequilibrium dynamics of a magnetic impurity coupled with metallic contacts. To highlight the importance of our formulation here we consider the simple case $V_g = h = 0$, and we take the wide-band limit (WBL). Moreover, we will firstly analyze the steady-state regime by computing the nonequilibrium ground-state and the differential conductance as a function of the voltage applied to the contacts. Then, we will study the out of equilibrium evolution induced by a slowly varying time-dependent voltage.

A. The steady-state solution in the wide band limit

Initially, we assume the dot disconnected by the leads, which are prepared at two different chemical potential

$\pm\phi/2$, so that their initial distribution function is described by Eq. (22). Once the tunneling amplitude is turned on, after the initial transient, the steady-state Hamiltonian, that describes the quantum pseudospin degree of freedom, is given by:

$$H_\sigma^* = -\frac{U}{4}\sigma^z + \langle T \rangle_{st}\sigma^x.$$

In the wide-band limit, where $\Gamma(\epsilon) = \Gamma_0$, the f electron self-energy reduces to

$$\Sigma_{f\sigma}^R(\omega) = -i2\Gamma_0 \sin^2 \theta, \quad (34)$$

and we readily find that

$$\langle T \rangle_{st} = -\frac{4\Gamma}{\pi \sin \theta} \log \frac{D}{\sqrt{\Gamma^2 + \phi^2/4}}, \quad (35)$$

where Γ is the renormalized hybridization amplitude $\Gamma = 2\Gamma_0 \sin^2 \theta$. The steady-state variational ground-state is obtained by solving the self-consistent equation:

$$\sin \theta = -\frac{4\langle T \rangle_{st}/U}{\sqrt{1 + (4\langle T \rangle_{st}/U)^2}}. \quad (36)$$

For large U , and $\phi \ll \Gamma$, the solution of the self-consistent Eq. (36) for Γ reads:

$$\Gamma(\phi) \simeq \Gamma(0) - \frac{\phi^2}{8\Gamma(0)}, \quad (37)$$

where

$$\Gamma(0) = D \exp \left[-\frac{\pi U}{16(2\Gamma_0)} \right]$$

is the same as in slave-boson mean-field theory, and can be associated with the Kondo temperature T_K , though overestimated respect its actual value⁴⁴. As shown in Eq. (37) the effect of an external voltage ϕ , within mean-field approximation, is to reduce the equilibrium value of the renormalized hybridization $\Gamma(0)$. Moreover, the mean-field steady-state breaks spontaneously the Z_2 gauge symmetry by choosing one of the two degenerate minima $\langle \sigma^x \rangle_{st} \neq 0$, as already observed in the equilibrium case Ref.⁴⁴.

At the steady-state variational minimum we can compute the average value of the current:

$$\langle I \rangle_{st} = -\frac{i}{\sqrt{2V}} \sum_{k\sigma} v_k \left(\langle c_{2k\sigma}^\dagger \sigma^x f_\sigma \rangle_{st} - c.c. \right) \quad (38)$$

that involves the evaluation of the two-particle correlation function $G_{x,2k\sigma}^<(t,t') = i\langle c_{2k\sigma}^\dagger(t')\sigma^x(t)f_\sigma(t) \rangle_{st}$. In a consistent approximation scheme the self-energy corrections have to be included in two-particle correlation functions through the Bethe-Salpeter equation. In the next section, by means of the Abrikosov representation⁴⁵ of the pseudospin variable σ , we readily compute the average value of the current (38) consistently with the mean-field approximation (24).

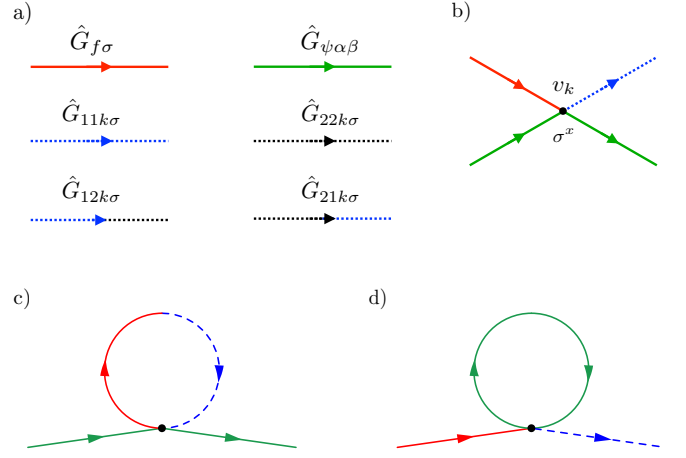


Figure 1. a) Bare Green's functions. b) Bare interaction. Hartree-Fock self-energy diagrams corresponding to the slave-spin mean-field approximation: c) elastic scattering between f_σ and $c_{1k\sigma}$ fermions renormalized by $\langle \psi_\alpha^\dagger \sigma_\alpha^x \psi_\beta \rangle$, d) ψ fermions self-energy determined by valence fluctuations induced by the hybridization operator T .

B. The steady-state current within a self-consistent mean-field approximation

To perform a self-consistent calculation of the current, Eq. (38), we introduce a couple of fermionic operators ψ corresponding to the pseudospin operator $\vec{\sigma}$ according to the formula⁴⁵:

$$\psi_\alpha^\dagger \sigma_\alpha^i \psi_\beta = \hat{\sigma}^i \quad (39)$$

where the upper index $i = 1, 2, 3$ denotes the Pauli matrices, while $\alpha, \beta = \pm$. The fermion substitution Eq. (39) introduces two additional configurations (0,0) and (1,1) to the two dimensional Hilbert space of the σ -matrices, which is composed by (1,0) and (0,1). However, in the case of spin $S = 1/2$ the unphysical configurations are automatically excluded since physical quantities involve only averages of products of $\hat{\sigma}^i$, which have the property of giving zero when acting on the non-physical states (0,0) or (1,1).

In this representation, the hybridization term in Eq. (4) becomes the four-leg fermionic interaction vertex depicted in Fig. 1 b). The Hartree-Fock approximation corresponds to the mean-field decoupling presented in section IV, and is described by the self-energy diagrams in Figs. 1 c) and d). The average value of the current reads:

$$\langle I \rangle_{st} = -\frac{i}{\sqrt{2V}} \sum_{k\sigma} v_k \left(\langle c_{2k\sigma}^\dagger \psi_\alpha^\dagger \sigma_\alpha^x \psi_\beta f_\sigma \rangle_{st} - c.c. \right)$$

and implies the evaluation of the two-particle correlation function $\langle c_{2k\sigma}^\dagger \psi_\alpha^\dagger \sigma_\alpha^x \psi_\beta f_\sigma \rangle_{st}$. Therefore, consistently with the slave-spin mean-field decoupling the current is made up of two contributions, Figs. 2 a) and b):

$$\langle I \rangle_{st} = \langle I_f \rangle_{st} + \langle \delta I \rangle_{st} \quad (40)$$

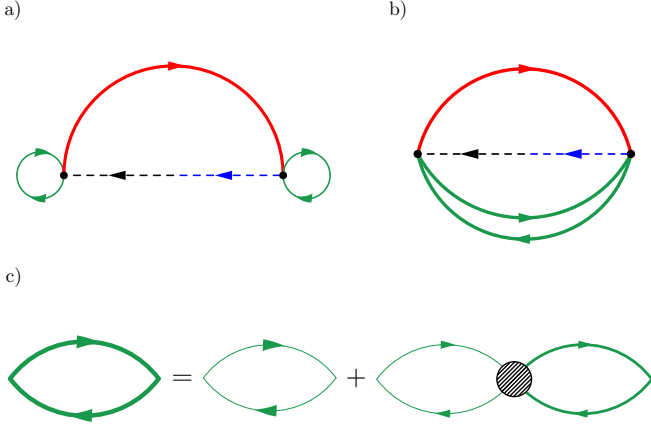


Figure 2. Feynman diagrams contributing to the average value of the current. Top panel: a) $\langle I_f \rangle_{st}$ low-energy contribution to the current given by a Resonant level model with renormalized hybridization amplitude, b) $\langle \delta I \rangle_{st}$ is determined by the convolution of the low-energy fermions with the valence fluctuations described by Π_{xx} . Lower panel: c) Dyson's Eq. for the Π_{xx} propagator.

where the former, $\langle I_f \rangle_{st}$, involves only the low-energy pseudofermion degree of freedom, and can be obtained by straightforward calculations summarized in appendix A. Here, we report the final result in the WBL:

$$\langle I_f \rangle_{st} = 2\Gamma(\phi) \frac{2e}{h} \arctan\left(\frac{e\phi}{2\Gamma(\phi)}\right), \quad (41)$$

where e is the elementary charge and h the Planck's constant.

Instead, the latter term in Eq. (40) takes into account the contribution of valence fluctuations and can be expressed as

$$\langle \delta I \rangle_{st} = -\frac{4\Gamma_0 e}{h} \int d\omega (f_L(\omega) - f_R(\omega)) \text{Re} \mathcal{K}(\omega) \quad (42)$$

where the kernel $\mathcal{K}(\omega)$ is given by:

$$\mathcal{K}(\omega) = \int \frac{d\epsilon}{2\pi} \left[\Pi_{xx}^<(\epsilon) G_f^R(\omega - \epsilon) + \Pi_{xx}^R(\epsilon) G_f^R(\omega - \epsilon) + \Pi_{xx}^R(\epsilon) G_f^<(\omega - \epsilon) \right],$$

where Π_{xx} is the ψ fermion spin-correlation function, for more details we refer to appendix B. Consistently with the Hartree-Fock approximation Π_{xx} satisfies the Dyson's Eq. in Fig. 2 c), whose solution for the retarded component reads:

$$\Pi_{xx}^R(\omega) = \frac{1}{\left[\Pi_{xx}^{0R}(\omega) \right]^{-1} - \Sigma_{xx}^R(\omega)}, \quad (43)$$

and the lesser component:

$$\Pi_{xx}^<(\omega) = \Pi_{xx}^R(\omega) \Sigma_{xx}^<(\omega) \Pi_{xx}^A(\omega), \quad (44)$$

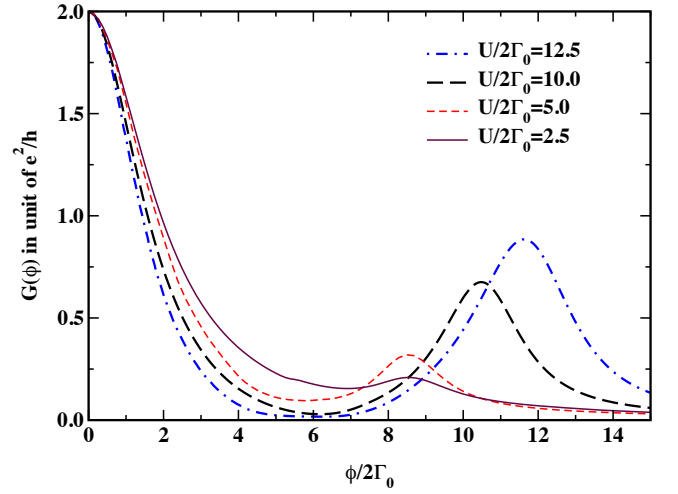


Figure 3. Differential conductance as a function of the applied voltage $\phi/2\Gamma_0$ for $U/D = 0.1$ and different hybridization amplitudes $2\Gamma_0$.

where $\Pi_{xx}^{0R}(\omega) = 2\omega_0 \cos^2 \theta / (\omega^2 - \omega_0^2)$ and $\Pi_{xx}^A(\omega) = [\Pi_{xx}^R(\omega)]^*$. The self-energies appearing in Eqs. (43) and (44) are obtained by contracting the four-leg vertex in Fig. 1 b), details can be found in appendix B. Specifically, the self-energy $\Sigma_{xx}(\omega)$ allows to reconstruct incoherent side bands characterized by a width of the order of the bare hybridization Γ_0 and centered around $\pm U/2$ as shown in Fig. 4.

Numerical integration of Eq. (42) permits to compute the differential conductance

$$G(\phi) = \frac{d\langle I \rangle_{st}}{d\phi},$$

which is shown in Fig. 3. We observe two distinct contributions: (i) the well-known zero-bias anomaly which derives from the Kondo peak at the Fermi level and controls the low-bias behavior and (ii) an incoherent one, which mainly contributes to the large bias features of the conductance.

To compare our result for $G(\phi)$ with the universal behavior of the conductance in the Kondo regime, obtained with renormalization group approach in Refs.^{46,47}, we expand $\langle I \rangle_{st}$ around $\phi/\Gamma \ll 1$ obtaining:

$$G(\phi) = \frac{2e^2}{h} \left[1 - \frac{1}{4} \left(\frac{\phi}{\Gamma} \right)^2 \right]. \quad (45)$$

In agreement with our self-consistent Hartree-Fock approximation, Eq.(45) reproduces exactly the ϕ^2 contribution given by the phase shift, while neglects the contribution from the residual scattering among low-energy quasiparticles⁴⁸. We believe that, in the slave-spin representation, the latter contribution comes from vertex corrections, that are not included in our perturbative calculation.

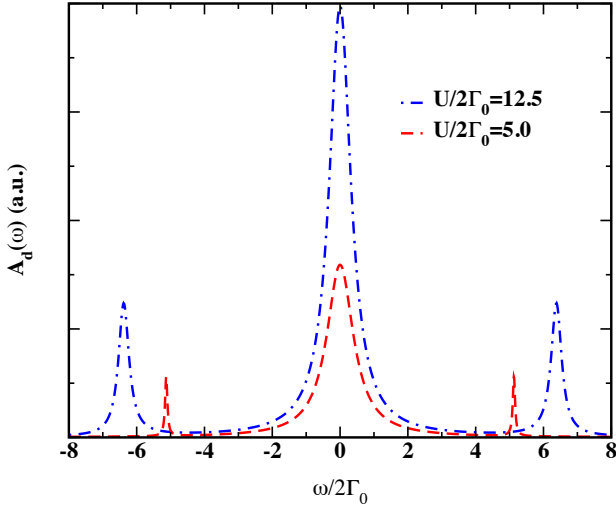


Figure 4. Physical d_σ electrons spectral function $A_d(\omega)$ computed at equilibrium, $\phi = 0$, for $U/D = 0.1$ and $U/2\Gamma_0 = 12.5, 5.0$. In addition to the low energy Abrikosov-Suhl or Kondo resonance $A_d(\omega)$ presents high energy side-bands.

C. Adiabatic dynamic induced by a time-dependent voltage

Physically, applying a time-dependent voltage between the source and the drain contacts means that the single-particle energies become time-dependent: $\epsilon_k \rightarrow \epsilon_k - \phi_a(t)$ (here a label refers to the left L or right R lead)⁴⁹. Starting, at $t = 0$, from an equilibrium configuration characterized by $\phi_L = \phi_R = 0$ ($N_L = N_R$) and a finite tunneling amplitude v_k , we consider the evolution induced by a time-dependent electrochemical potential:

$$\phi_L(t) = \theta(t)\phi \frac{1 - e^{-t/t^*}}{2}, \quad \phi_R(t) = -\phi_L(t), \quad (46)$$

where t^* is the characteristic time scale of the external perturbation, ϕ is the asymptotic value of the voltage and $\theta(t)$ is the Heaviside step function such that $\phi_L(t) = 0$ for $t \leq 0$. Here we consider the WBL analogously to the steady-state analysis. The dynamic of the pseudospin variable is:

$$\begin{aligned} \partial_t \langle \sigma^x(t) \rangle &= U \langle \sigma^y(t) \rangle / 2, \\ \partial_t \langle \sigma^y(t) \rangle &= -2 \langle T(t) \rangle \langle \sigma^z(t) \rangle - U \langle \sigma^x(t) \rangle / 2, \\ \partial_t \langle \sigma^z(t) \rangle &= 2 \langle T(t) \rangle \langle \sigma^y(t) \rangle, \end{aligned} \quad (47)$$

where the time-dependent average value of the hybridization is given by:

$$\langle T(t) \rangle = \frac{2}{\langle \sigma^x(t) \rangle} \text{Im} \left[\int \frac{d\epsilon}{\pi} \Sigma_f^<(t, \epsilon) \star G_f^A(t, \epsilon) \right]. \quad (48)$$

In this case (48), the normal product is substituted with $\star = \exp \left[i(\overleftarrow{\partial}_\epsilon \overrightarrow{\partial}_t - \overleftarrow{\partial}_t \overrightarrow{\partial}_\epsilon) / 2 \right]$, while $\Sigma_f^<(t, \epsilon)$ and $G_f^A(t, \epsilon)$ are the Wigner transform of the lesser component of the self-energy and the advanced Green's function

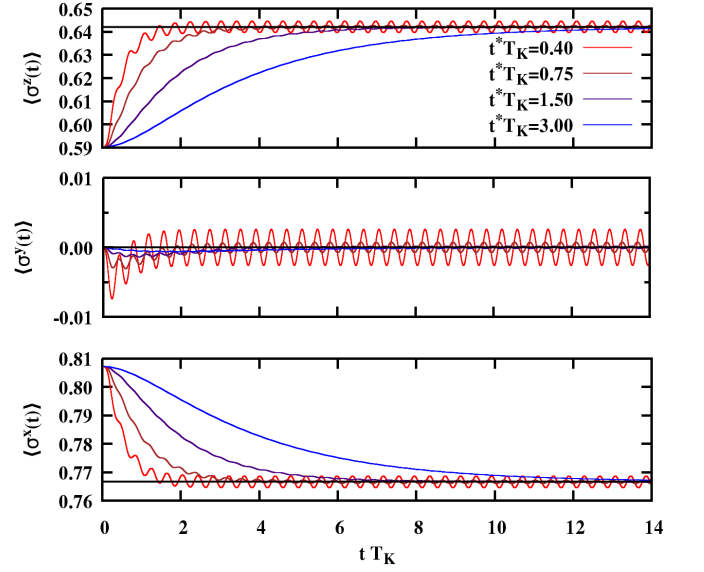


Figure 5. From top to bottom: evolution of $\langle \sigma^z(t) \rangle$, $\langle \sigma^y(t) \rangle$ and $\langle \sigma^x(t) \rangle$ as a function of $t T_K$ for several values of the external voltage time scale t^* , $U/D = 0.1$, $2\Gamma_0/U = 0.06$ and $\phi/U = 0.05$. Solid black line represents the steady-state result for the same set of parameters.

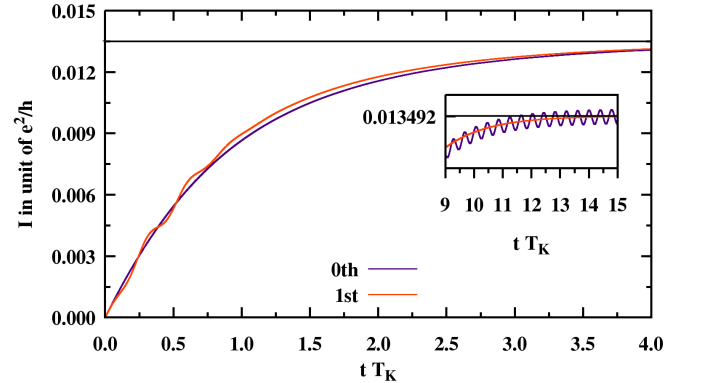


Figure 6. Time-dependent average value of the current as a function of $t T_K$ for $t^* T_K = 1.5$, $U/D = 0.1$, $2\Gamma_0/U = 0.06$ and $\phi/U = 0.05$. Orange and purple lines represent the evolution of the current obtained within first and second order in the gradient expansion. As shown from the inset, first order corrections to the quasistatic approximation introduce relaxation processes that suppress the residual oscillations.

of the f_σ pseudofermions, for more details we refer to appendix C.

In the following, we consider an external perturbation $\phi(t)$, which is a slowly varying function of time compared to the characteristic scales of the equilibrium state, i.e. $t^* T_K \gg 1$. Therefore, we can assume that the temporal inhomogeneity is weak and only lowest-order terms in the variation are kept, the so-called gradient expansion^{40,41}. To the first-order in the temporal variation we have:

$$\begin{aligned}
\langle T(t) \rangle &\simeq \frac{2}{\langle \sigma^x(t) \rangle} \text{Im} \int \frac{d\epsilon}{\pi} \left[\Sigma_f^<(t, \epsilon) G_f^A(t, \epsilon) \right. \\
&\quad \left. + \frac{i}{2} \left\{ \Sigma_f^<(t, \epsilon), G_f^A(t, \epsilon) \right\}_{\epsilon, t} \right] \\
&= \langle T(t) \rangle^{(0)} + \langle T(t) \rangle^{(1)}
\end{aligned} \tag{49}$$

where $\{f, g\}_{\epsilon, t} = \partial_\epsilon f \partial_t g - \partial_t f \partial_\epsilon g$, more details can be found in Appendix C.

The evolution of the pseudospin variable induced within the zeroth order in the gradient expansion Eq. (49) is displayed in Fig. 5. In the limit of $t^* T_K \gg 1$ we observe, as expected, the quasistatic dynamic, i.e. the system stays in equilibrium at all times and follows the change of $\mu(t)$ adiabatically. However, for any smaller value of $t^* T_K$ the dynamics is characterized by persistent oscillations, that become, eventually, centered around the steady-state result represented by the solid black line.

Remarkably, first-order correction, given by the latter term in Eq. (49), introduces a relaxation mechanism and the dynamic converges to the expected stationary regime. This is shown in Fig. 6, where we compare the time-dependent average value of the current obtained within the zeroth and first order in the gradient expansion.

VI. CONCLUSIONS

We have shown that the out of equilibrium evolution of a single-orbital AIM (1) can be calculated in the slave-spin representation (12) without any constraint on the enlarged Hilbert space. The advantages of the new representation are twofold. On one side, we disentangle charge and spin degrees of freedom. On the other side, we avoid the mean-field mixing of unphysical and physical subspaces, that affects the time evolution of other slave-particle techniques. In the steady-state regime the self-consistent Hartree-Fock decoupling is able to predict properties of the model even deep inside the large- U Kondo regime, specifically, the conductance shows both the known zero-bias anomaly but also the expected peak at bias of order U . Furthermore, we have extended the slave-spin approach to study the transient dynamic of a driven magnetic impurity. By means of a time-dependent Hartree-Fock calculation, in the adiabatic regime, we prove that, at first-order in the gradient expansion, the current relaxes to the steady state value after an initial transient.

Finally, we mention that the technique we have proposed can be applied to study the out of equilibrium dynamics of multi-orbitals magnetic impurities by using the generalized mapping presented in Ref.³⁸.

ACKNOWLEDGMENTS

I am grateful to Michele Fabrizio for insightful discussions that allowed me to clarify several important points

related to this work and for a careful reading of this manuscript. Furthermore, I thank Roberto Raimondi, Francesco Grandi, Massimo Capone, Laura Fanfarillo, Valentina Brosco, Maria Florencia Ludovico and Adriano Amaricci for constructive discussions on the manuscript. We acknowledge support from the H2020 Framework Programme under ERC Advanced Grant No. 692670 FIRSTORM.

Appendix A: The effective Resonant level model in the steady-state regime

In this section we derive analytic expressions for the hybridization Eq. (26) and the current Eq. (41). Moreover, we compute the Keldysh's components of the f_σ and ψ fermion Green's function within Hartree-Fock approximation.

a. f_σ pseudofermion Green's function The unperturbed retarded and advanced Green's functions of the contacts are

$$\begin{aligned}
G_{11\sigma}^{R/A}(\epsilon, k) &= G_{22\sigma}^{R/A}(\epsilon, k) = \frac{1}{\epsilon - \epsilon_k \pm i0^+}, \\
G_{12\sigma}^{R/A}(\epsilon, k) &= G_{21\sigma}^{R/A}(\epsilon, k) = 0,
\end{aligned}$$

and

$$\begin{aligned}
G_{11\sigma}^<(\epsilon, k) &= G_{22\sigma}^<(\epsilon, k) = 2i\pi\delta(\epsilon - \epsilon_k) \frac{f_L(\epsilon) + f_R(\epsilon)}{2}, \\
G_{12\sigma}^<(\epsilon, k) &= G_{21\sigma}^<(\epsilon, k) = 2i\pi\delta(\epsilon - \epsilon_k) \frac{f_L(\epsilon) - f_R(\epsilon)}{2},
\end{aligned}$$

where we have already performed the rotation in Eq. (8). In terms of the matrix representation

$$\hat{G} = \begin{pmatrix} G^R & G^< \\ 0 & G^A \end{pmatrix} \tag{A1}$$

the Dyson's equation for the f_σ pseudofermion Green's function on the Keldysh's contour is:

$$\hat{G}_{f\sigma} = \hat{G}_{f\sigma}^0 + \hat{G}_{f\sigma}^0 \cdot \hat{\Sigma}_f \cdot \hat{G}_{f\sigma} \tag{A2}$$

where $\hat{G}_{f\sigma}$ is the dressed Green's function and $\hat{G}_{f\sigma}^0$ the unperturbed one. In Eq. (A2) we use a notation where the product \cdot is interpreted as a matrix product in the internal variables (time and Keldysh's indices). In the stationary regime the time translational invariance is restored, thus, by taking the Fourier transform of Eq. (A2) we obtain:

$$G_{f\sigma}^{R/A}(\epsilon) = \frac{1}{\epsilon + \lambda_\sigma - \Sigma_{f\sigma}^{R/A}(\epsilon)} \tag{A3}$$

and

$$G_{f\sigma}^<(\epsilon) = G_{f\sigma}^A(\epsilon) \Sigma_{f\sigma}^<(\epsilon) G_{f\sigma}^R(\epsilon). \tag{A4}$$

Within mean-field approximation the self-energy of the $\Sigma_{f\sigma}$ reads:

$$\begin{aligned}\Sigma_{f\sigma}^{R/A}(\epsilon) &= \langle \sigma^x \rangle_{st}^2 \frac{2}{V} \sum_k v_k^2 G_{11\sigma}^{R/A}(\epsilon, k) \\ &= 2 \langle \sigma^x \rangle_{st}^2 \int \frac{d\omega}{\pi} \frac{\Gamma(\omega)}{\epsilon - \omega \pm i0^+}\end{aligned}$$

and

$$\begin{aligned}\Sigma_{f\sigma}^<(\epsilon) &= \langle \sigma^x \rangle_{st}^2 \frac{2}{V} \sum_k v_k^2 G_{11\sigma}^<(\epsilon, k) \\ &= 4 \langle \sigma^x \rangle_{st}^2 i\Gamma(\epsilon) f_{\text{neq}}(\epsilon).\end{aligned}\quad (\text{A5})$$

b. Expectation values The average occupation on the quantum dot (32) follows from Eqs. (A4) and (A5). The average value of the hybridization (26) involves the lesser component of the mixed Green's function:

$$G_{1kf\sigma}^< = \sqrt{\frac{2}{V}} v_k \langle \sigma^x \rangle_{st} [\hat{G}_{11k\sigma} \cdot \hat{G}_{f\sigma}]^<. \quad (\text{A6})$$

Thus,

$$\langle T \rangle_{st} = \frac{2}{\langle \sigma^x \rangle_{st}} \sum_{\sigma} \int \frac{d\epsilon}{2\pi} \text{Im} [\hat{\Sigma}_{f\sigma}(\epsilon) \cdot \hat{G}_{f\sigma}(\epsilon)]^<. \quad (\text{A7})$$

By using Eqs. (A3), (A4) and (A5) we readily obtain Eq. (31) reported in the main text. Finally, we briefly derive the expression for the low-energy contribution to the current average value Eq. (41). In this case the mixed Green's function involved is $G_{2kf\sigma}^<(t, t) = i \langle f_{\sigma}^{\dagger}(t) c_{2k\sigma}(t) \rangle_{st}$ and its Dyson's equation reads:

$$G_{2kf\sigma}^<(\epsilon) = \sqrt{\frac{2}{V}} v_k \langle \sigma^x \rangle_{st} G_{21k\sigma}^<(\epsilon) G_{f\sigma}^A(\epsilon).$$

The average value of the current is:

$$\langle I_f \rangle_{st} = \sum_{\sigma} \int \frac{d\epsilon}{2\pi} \text{Re} [\Sigma_{21\sigma}^<(\epsilon) G_{f\sigma}^A(\epsilon)], \quad (\text{A8})$$

where

$$\begin{aligned}\Sigma_{21\sigma}^<(\epsilon) &= \langle \sigma^x \rangle_{st}^2 \frac{2}{V} \sum_k v_k^2 G_{21k\sigma}^<(\epsilon) \\ &= 4 \langle \sigma^x \rangle_{st}^2 i\Gamma(\epsilon) \frac{f_L(\epsilon) - f_R(\epsilon)}{2}.\end{aligned}$$

In the WBL Eq. (A8) gives Eq. (41).

c. ψ fermion Green's function The Dyson's equation for the ψ fermion reads:

$$\hat{G}_{\psi} = \hat{G}_{\psi}^0 + \hat{G}_{\psi}^0 \cdot \hat{\Sigma}_{\psi} \cdot \hat{G}_{\psi}, \quad (\text{A9})$$

where the Hartree-Fock self-energy, depicted in Fig. 1 c) is:

$$\hat{\Sigma}_{\psi} = \sigma^x \langle T \rangle_{st},$$

In Eq. (A9) we are using the same notation introduced in Eq. (A2), where the hat refers to the matrix structure (A1). By performing straightforward calculations we obtain:

$$G_{\psi}^{R(A)}(\epsilon) = \sum_{\mu} \sigma^{\mu} G_{\psi\mu}^{R(A)}(\epsilon),$$

where $\mu = 0$ denotes the identity and $\mu = 1, 2, 3$ the remaining Pauli matrices, while $G_{\psi 2}^{R(A)}(\epsilon) = 0$ and

$$\begin{aligned}G_{\psi 0}^{R(A)}(\epsilon) &= \frac{1}{2} \left(\frac{1}{\epsilon + \omega_0/2 \pm i0^+} + \frac{1}{\epsilon - \omega_0/2 \pm i0^+} \right), \\ G_{\psi 1}^{R(A)}(\epsilon) &= \frac{\sin \theta}{2} \left(\frac{1}{\epsilon + \omega_0/2 \pm i0^+} - \frac{1}{\epsilon - \omega_0/2 \pm i0^+} \right), \\ G_{\psi 3}^{R(A)}(\epsilon) &= \frac{\cos \theta}{2} \left(\frac{1}{\epsilon + \omega_0/2 \pm i0^+} - \frac{1}{\epsilon - \omega_0/2 \pm i0^+} \right),\end{aligned}$$

with $\omega_0 = U \sqrt{1 + 16 \langle T \rangle_{st}^2 / U^2} / 2$ and θ solution of Eq. (33). Finally, we report the lesser component:

$$G_{\psi}^<(\epsilon) = \sum_{\mu} \sigma^{\mu} G_{\psi\mu}^<(\epsilon),$$

where $G_{\psi 2}^<(\epsilon) = 0$ and

$$\begin{aligned}G_{\psi 0}^<(\epsilon) &= i\pi f(\epsilon) [\delta(\epsilon + \omega_0/2) + \delta(\epsilon - \omega_0/2)], \\ G_{\psi 1}^<(\epsilon) &= i\pi f(\epsilon) \sin \theta [\delta(\epsilon + \omega_0/2) - \delta(\epsilon - \omega_0/2)], \\ G_{\psi 3}^<(\epsilon) &= i\pi f(\epsilon) \cos \theta [\delta(\epsilon + \omega_0/2) - \delta(\epsilon - \omega_0/2)].\end{aligned}$$

Appendix B: RPA corrections to the spin correlation function

In this section, we compute the RPA correction to the σ^x mode, which describes valence fluctuations on the impurity site. In terms of the fermionic representation introduced in Eq. (39) the bare Π_{xx} propagator reads:

$$\hat{\Pi}_{xx}^0(t, t') = -i \text{Tr} [\sigma^x \hat{G}_{\psi}(t, t') \sigma^x \hat{G}_{\psi}(t', t)],$$

where \hat{G}_{ψ} is the Hartree-Fock ψ fermion Green's function in Eq. (A9). As shown in Fig. 2 c) the Dyson's equation reads:

$$\hat{\Pi}_{xx} = \hat{\Pi}_{xx}^0 + \hat{\Pi}_{xx}^0 \cdot \hat{\Sigma}_{xx} \cdot \hat{\Pi}_{xx},$$

where we adopt the notation introduced in Eq. (A1). At RPA level the bosonic self-energy reads:

$$\hat{\Sigma}_{xx} = \hat{\chi}_{TT}, \quad (\text{B1})$$

with:

$$\chi_{TT}(t, t') = -i \langle T_C(\delta T(t) \delta T(t')) \rangle$$

where $\delta T = T - \langle T \rangle_{st}$, and T is the hybridization operator in Eq. (4). Within the WBL, introduced in Eq. (34), the

evaluation of the bosonic self-energy (B1) is considerably simplified. We find:

$$\begin{aligned}\chi_{TT}^<(\omega) = & -i \frac{1}{\pi \langle \sigma^x \rangle_{st}^2} \int d\epsilon \left[G_f^<(\epsilon + \omega) \Sigma_f^>(\epsilon) \right. \\ & \left. + \Sigma_f^<(\epsilon + \omega) G_f^>(\epsilon) \right] \\ & - i \frac{2}{\pi \langle \sigma^x \rangle_{st}^2} \int d\epsilon \Sigma_f^<(\epsilon + \omega) \Sigma_f^>(\epsilon) \\ & \text{Re} \left[G_f^R(\epsilon + \omega) G_f^R(\epsilon) \right],\end{aligned}$$

and

$$\begin{aligned}\chi_{TT}^R(\omega) = & -i \frac{1}{\pi \langle \sigma^x \rangle_{st}^2} \int d\epsilon \Sigma_f^<(\epsilon) \left[G_f^R(\epsilon + \omega) \right. \\ & \left. + G_f^A(\epsilon - \omega) \right] \\ & - i \frac{2\Sigma_f^R}{\pi \langle \sigma^x \rangle_{st}^2} \int d\epsilon \Sigma_f^<(\epsilon) \\ & \left[G_f^R(\epsilon + \omega) G_f^R(\epsilon) - G_f^A(\epsilon - \omega) G_f^A(\epsilon) \right].\end{aligned}$$

Appendix C: Transient dynamics of the effective Resonant level model

The dynamics of the spin degree of freedom is influenced by the time-dependent expectation value of the hybridization Eq. (48). By assuming a slowly varying electrochemical potential (46), we compute Eq. (48) to the first-order in the gradient expansion Eq. (49). To this aim we define the Wigner transform of the f_σ pseudofermion Green's function:

$$G_{f\sigma}^{R(A)}(t, \epsilon) = \int d\tau e^{i\epsilon\tau} G_{f\sigma}^{R(A)}\left(t + \frac{\tau}{2}, t - \frac{\tau}{2}\right),$$

which satisfies the Dyson's equation:

$$\left(\epsilon - \Sigma_{f\sigma}^{R(A)}(t, \epsilon)\right) \star G_{f\sigma}^{R(A)}(t, \epsilon) = 1$$

where \star denotes the Moyal product introduced in the main text. The solution of the Dyson's equation up to first-order is:

$$G_{f\sigma}^{R(A)}(t, \epsilon) = \frac{1}{\epsilon - \Sigma_{f\sigma}^{R(A)}(t, \epsilon)}$$

where in the WBL the time-dependent self-energy is $\Sigma_{f\sigma}^{R(A)}(t, \epsilon) = \mp 2i\Gamma_0 \langle \sigma^x(t) \rangle^2$. Instead, the lesser self-

energy is given by:

$$\begin{aligned}\Sigma_{f\sigma}^<(t, \epsilon) = & 2i\Gamma_0 \langle \sigma^x(t) \rangle^2 - \frac{2\Gamma_0}{\pi} \int d\tau \frac{e^{i\epsilon\tau}}{\tau} \\ & \cos \gamma(t, \tau) \left\langle \sigma^x\left(t + \frac{\tau}{2}\right) \right\rangle \left\langle \sigma^x\left(t - \frac{\tau}{2}\right) \right\rangle \quad (\text{C1}) \\ & \simeq 4\Gamma_0 i \langle \sigma^x(t) \rangle^2 f_{\text{neq}}(t, \epsilon),\end{aligned}$$

where $\gamma(t, \tau) = \int_{t-\tau/2}^{t+\tau/2} \mu_L(x) dx$ and the nonequilibrium distribution reads

$$f_{\text{neq}}(t, \epsilon) = \frac{1}{2} + \frac{i}{2\pi} \int d\tau \frac{e^{i\epsilon\tau}}{\tau} \cos \gamma(t, \tau).$$

In the last passage of Eq. (C1), we assume that the dependence of $\langle \sigma^x(t) \rangle$ on the relative time τ is negligible.

In the following, we report the zeroth and first-order contributions to the gradient expansion of $\langle T(t) \rangle$.

a. Zeroth order The zeroth order contribution, first term in Eq. (49), reads:

$$\langle T(t) \rangle^{(0)} = \frac{4}{\langle \sigma^x(t) \rangle} \int d\epsilon A_f(t, \epsilon) \epsilon f_{\text{neq}}(t, \epsilon),$$

where the f_σ pseudofermion time-dependent spectral function is

$$A_f(t, \epsilon) = \frac{1}{\pi} \frac{\Gamma(t)}{\epsilon^2 + \Gamma(t)^2},$$

with $\Gamma(t) = 2\Gamma_0 \langle \sigma^x(t) \rangle^2$.

b. First order The first order correction to the quasistatic approximation is the second term of Eq. (49), which reads:

$$\begin{aligned}\langle T(t) \rangle^{(1)} = & \frac{1}{\pi \langle \sigma^x(t) \rangle} \text{Im} \int d\epsilon \left[i \left(\partial_\epsilon \Sigma_f^<(t, \epsilon) \partial_t \Sigma_f^A(t, \epsilon) \right. \right. \\ & \left. \left. + \partial_t \Sigma_f^<(t, \epsilon) \right) G_f^A(t, \epsilon)^2 \right].\end{aligned}$$

After straightforward calculations we obtain

$$\begin{aligned}\langle T(t) \rangle^{(1)} = & -\frac{2\Gamma(t)}{\pi \langle \sigma^x(t) \rangle} \int d\epsilon \left[\text{Im} \left[G_f^A(t, \epsilon)^2 \right] \partial_t f_{\text{neq}}(t, \epsilon) \right. \\ & + 2 \frac{\partial_t \langle \sigma^x(t) \rangle}{\langle \sigma^x(t) \rangle} \left(f_{\text{neq}}(t, \epsilon) \text{Im} \left[G_f^A(t, \epsilon)^2 \right] \right. \\ & \left. \left. + \partial_\epsilon f_{\text{neq}}(t, \epsilon) \Gamma(t) \text{Re} \left[G_f^A(t, \epsilon)^2 \right] \right) \right].\end{aligned}$$

Since $\partial_t \langle \sigma^x(t) \rangle = U \langle \sigma^y(t) \rangle / 2$ the latter contribution modifies the Heisenberg equation (47) by introducing a finite relaxation in the evolution of the $\langle \sigma^y(t) \rangle$ component.

¹ A. C. Hewson, *The Kondo Problem to Heavy Fermions*, Cambridge Studies in Magnetism (Cambridge University Press, 1993).

² J. Kondo, Progress of Theoretical Physics **32**, 37 (1964), URL <http://dx.doi.org/10.1143/PTP.32.37>.

- ³ P. W. Anderson, *Journal of Physics C: Solid State Physics* **3**, 2436 (1970), URL <http://stacks.iop.org/0022-3719/3/i=12/a=008>.
- ⁴ F. Stefan, J. Martínez-Blanco, J. Yang, K. Kanisawa, and S. C. Erwin, *Nature Nanotechnology* **9**, 505 (2014), URL <https://doi.org/10.1038/nnano.2014.129>.
- ⁵ J. Martínez-Blanco, C. Nacci, S. C. Erwin, K. Kanisawa, E. Locane, M. Thomas, F. von Oppen, P. W. Brouwer, and F. Stefan, *Nature Physics* **11**, 640 (2015), URL <https://doi.org/10.1038/nphys3385>.
- ⁶ Y. Pan, J. Yang, S. C. Erwin, K. Kanisawa, and S. Fölsch, *Phys. Rev. Lett.* **115**, 076803 (2015), URL <https://link.aps.org/doi/10.1103/PhysRevLett.115.076803>.
- ⁷ M. A. Kastner, *Physics Today* **46**, 24 (1993), URL <https://doi.org/10.1063/1.881393>.
- ⁸ R. C. Ashoori, *Nature* **379**, 413 (1996), URL <https://doi.org/10.1038/379413a0>.
- ⁹ D. Goldhaber-Gordon, J. Göres, M. A. Kastner, H. Shtrikman, D. Mahalu, and U. Meirav, *Phys. Rev. Lett.* **81**, 5225 (1998).
- ¹⁰ S. M. Cronenwett, T. H. Oosterkamp, and L. P. Kouwenhoven, *Science* **281**, 540 (1998), <http://www.sciencemag.org/cgi/reprint/281/5376/540.pdf>, URL <http://www.sciencemag.org/cgi/content/abstract/281/5376/540>.
- ¹¹ L. I. Glazman and M. E. Raikh, *JETP Lett.* **47**, 452 (1988).
- ¹² T. K. Ng and P. A. Lee, *Phys. Rev. Lett.* **61**, 1768 (1988).
- ¹³ T. Kobayashi, S. Tsuruta, S. Sasaki, T. Fujisawa, Y. Tokura, and T. Akazaki, *Phys. Rev. Lett.* **104**, 036804 (2010), URL <https://link.aps.org/doi/10.1103/PhysRevLett.104.036804>.
- ¹⁴ F. B. Anders and A. Schiller, *Phys. Rev. Lett.* **95**, 196801 (2005), URL <http://link.aps.org/abstract/PRL/v95/e196801>.
- ¹⁵ F. B. Anders and A. Schiller, *Phys. Rev. B* **74**, 245113 (2006).
- ¹⁶ F. B. Anders, *Phys. Rev. Lett.* **101**, 066804 (2008), URL <https://link.aps.org/doi/10.1103/PhysRevLett.101.066804>.
- ¹⁷ P. Werner, T. Oka, and A. J. Millis, *Phys. Rev. B* **79**, 035320 (2009).
- ¹⁸ M. Schiró and M. Fabrizio, *Phys. Rev. B* **79**, 153302 (2009), URL <https://link.aps.org/doi/10.1103/PhysRevB.79.153302>.
- ¹⁹ S. R. White and A. E. Feiguin, *Phys. Rev. Lett.* **93**, 076401 (2004), URL <https://link.aps.org/doi/10.1103/PhysRevLett.93.076401>.
- ²⁰ P. Schmitteckert, *Phys. Rev. B* **70**, 121302(R) (2004), URL <https://link.aps.org/doi/10.1103/PhysRevB.70.121302>.
- ²¹ E. Boulat, H. Saleur, and P. Schmitteckert, *Phys. Rev. Lett.* **101**, 140601 (2008).
- ²² S. Kehrein, *Phys. Rev. Lett.* **95**, 056602 (2005), URL <https://link.aps.org/doi/10.1103/PhysRevLett.95.056602>.
- ²³ P. Fritsch and S. Kehrein, *Phys. Rev. B* **81**, 035113 (2010).
- ²⁴ C. Tomaras and S. Kehrein, *EPL (Europhysics Letters)* **93**, 47011 (2011), URL <http://stacks.iop.org/0295-5075/93/i=4/a=47011>.
- ²⁵ P. Nordlander, M. Pustilnik, Y. Meir, N. S. Wingreen, and D. C. Langreth, *Phys. Rev. Lett.* **83**, 808 (1999), URL <https://link.aps.org/doi/10.1103/PhysRevLett.83.808>.
- ²⁶ A. Kaminski, Y. V. Nazarov, and L. I. Glazman, *Phys. Rev. B* **62**, 8154 (2000).
- ²⁷ A. Rosch, J. Paaske, J. Kroha, and P. Wölffe, *Phys. Rev. Lett.* **90**, 076804 (2003).
- ²⁸ W. Metzner, M. Salmhofer, C. Honerkamp, V. Meden, and K. Schönhammer, *Rev. Mod. Phys.* **84**, 299 (2012), URL <https://link.aps.org/doi/10.1103/RevModPhys.84.299>.
- ²⁹ H. Schoeller, *The European Physical Journal Special Topics* **168**, 179 (2009), ISSN 1951-6401, URL <https://doi.org/10.1140/epjst/e2009-00962-3>.
- ³⁰ Y. Ashida, T. Shi, M. C. Bañuls, J. I. Cirac, and E. Demler, *Phys. Rev. Lett.* **121**, 026805 (2018), URL <https://link.aps.org/doi/10.1103/PhysRevLett.121.026805>.
- ³¹ N. Lanatà and H. U. R. Strand, *Phys. Rev. B* **86**, 115310 (2012), URL <https://link.aps.org/doi/10.1103/PhysRevB.86.115310>.
- ³² R. Citro and F. Romeo, *Journal of Physics: Conference Series* **696**, 012014 (2016), URL <http://stacks.iop.org/1742-6596/696/i=1/a=012014>.
- ³³ M. F. Ludovico and M. Capone, *Phys. Rev. B* **98**, 235409 (2018), URL <https://link.aps.org/doi/10.1103/PhysRevB.98.235409>.
- ³⁴ B. Dong and X. L. Lei, *Phys. Rev. B* **63**, 235306 (2001), URL <https://link.aps.org/doi/10.1103/PhysRevB.63.235306>.
- ³⁵ R. Raimondi and P. Schwab, *Superlattices and Microstructures* **25**, 1141 (1999), ISSN 0749-6036, URL <http://www.sciencedirect.com/science/article/pii/S0749603699907231>.
- ³⁶ P. Mehta and N. Andrei, *Phys. Rev. Lett.* **96**, 216802 (2006).
- ³⁷ C. J. Bolech and N. Shah, *Phys. Rev. B* **93**, 085441 (2016), URL <https://link.aps.org/doi/10.1103/PhysRevB.93.085441>.
- ³⁸ D. Guerci and M. Fabrizio, *Phys. Rev. B* **96**, 201106(R) (2017), URL <https://link.aps.org/doi/10.1103/PhysRevB.96.201106>.
- ³⁹ M. Schiró and M. Fabrizio, *Phys. Rev. Lett.* **105**, 076401 (2010), URL <http://link.aps.org/doi/10.1103/PhysRevLett.105.076401>.
- ⁴⁰ J. Rammer, *Quantum Field Theory of Nonequilibrium States* (Cambridge University Press, 2007).
- ⁴¹ H. Haug and A. P. Jauho, *Quantum Kinetics in Transport and Optics of Semiconductors* (Springer, 1996).
- ⁴² P. I. Arseev, *Phys. Usp.* **58**, 1159 (2015), URL <https://ufn.ru/en/articles/2015/12/b/>.
- ⁴³ N. Lanatà, *Phys. Rev. B* **82**, 195326 (2010), URL <https://link.aps.org/doi/10.1103/PhysRevB.82.195326>.
- ⁴⁴ P. P. Baruselli and M. Fabrizio, *Phys. Rev. B* **85**, 073106 (2012), URL <http://link.aps.org/doi/10.1103/PhysRevB.85.073106>.
- ⁴⁵ A. A. Abrikosov, *Physics Physique Fizika* **2**, 5 (1965), URL <https://link.aps.org/doi/10.1103/PhysicsPhysiqueFizika.2.5>.
- ⁴⁶ M. Pustilnik and L. Glazman, *Journal of Physics: Condensed Matter* **16**, R513 (2004), URL <http://stacks.iop.org/0953-8984/16/i=16/a=R01>.
- ⁴⁷ E. Sela, Y. Oreg, F. von Oppen, and J. Koch, *Phys. Rev. Lett.* **97**, 086601 (2006), URL <https://link.aps.org/doi/10.1103/PhysRevLett.97.086601>.
- ⁴⁸ P. Nozières, *Journal of Low Temperature Physics* **17**, 31 (1974).

- ⁴⁹ A.-P. Jauho, N. S. Wingreen, and Y. Meir, Phys. Rev. B **50**, 5528 (1994), URL <https://link.aps.org/doi/10.1103/PhysRevB.50.5528>.